

A pareto-optimal approach to numerical scheme design for conservation laws

Romit Maulik and Gary G. Yen, *Fellow, IEEE*

Abstract—Most discrete approximations to first and second order derivatives in governing laws are generally designed through the Taylor’s series polynomials as well as the well known modified wavenumber analysis approach of Lele [1]. The base philosophy of the latter is characterized by a minimization of the dispersive error of the scheme (in essence the error in representing spectral quantities accurately). In addition, it is also desired to obtain suitable amounts of dissipation within a scheme so that signals of derivatives remain viable for nonlinear wave propagation. This problem of maximizing dispersion while minimizing (or maximizing) dissipation has generally been studied as an analytical optimization problem by previous researchers. Throughout the vast body of computational physics literature, to our knowledge, there has been no investigation of this framework within a pareto-optimal paradigm that gives the user access to desired combinations of these two competing objectives. This study aims to obtain pareto fronts for multiple coefficients of a stencil that evaluates the first order derivative and to test their viability for a nonlinear wave propagation problem given by the Burgers equation. Through our efforts we aim to construct a framework for scheme design with user-specified constraints and possibly competing objectives.

I. INTRODUCTION

THE seminal work of Lele [1] enabled the first systematic numerical scheme design paradigm for conservation laws with spectral-like accuracy. Since then, numerous researchers have framed optimization problems for scheme discovery to preserve some desirable characteristics of their numerically determined first and second order derivatives. Within the computational aeroacoustics community, it is desired that the numerical scheme design accurately represent the advection of the highest wavenumbers (or spatial frequencies) due to the nonlinear terms in the governing conservation laws. For the direct numerical simulation (DNS) community (primarily associated with solving the Navier-Stokes equations for fluid flow), spectral-like accuracy is desired for the reduction of resolution requirement as it is widely known that the effective resolution of a numerical scheme relates to number of grid points per wavelength of the shortest wave component [2]. For the latter, while the Nyquist sampling criterion may be satisfied for the instantaneous field values, inaccuracies at the highest wavenumbers may necessitate a much larger number of points for effective physics preservation. At the same time, order of truncation is important for rigorous validation of discrete schemes converging (eventually) to their underlying partial differential equations.

This study is motivated by the concepts put forth by Tam and Webb [3] where a dispersion error in a seven-point stencil is minimized at the expense of a reduction in the order of convergence of the scheme. In this celebrated study, the goal was to optimize for the dispersion relationship only, while zero dissipation was built into the optimization through the use of symmetric stencils thus catering to the demands of the DNS community. The immense computational cost of DNS precludes its use as an engineering tool and research efforts have been dedicated towards the development of large eddy simulation (LES) [4] techniques which compute the evolution of the largest scales (or eddies) in a solution field while modeling the effect of the highest wavenumbers. While there are many approaches to the modeling of these finer scales, one modern approach is the use of numerical discretizations with dissipative errors at higher wavenumbers to model the (generally) dissipative effect of the largest scales. This is in accordance with Kolmogorov theory for three-dimensional turbulence where it is generally accepted that the highest scales are dominated by the dissipative effective of molecular viscosity [5]. Thus, a significant portion of the LES community investigates the development of dissipative schemes for the purpose of implicit turbulence modeling (refer for instance [6] and references therein). In this work, we pose dissipation as an added objective to be optimized for, using a multiobjective optimization strategy given by the famous non-dominated sorting based genetic algorithm ideology (NSGA II) [7]. Our desired dissipation is specified as a constraint at the grid cutoff wavenumber. Through this investigation, we propose a multiobjective framework that may be utilized for scheme design given a set of a-priori chosen performance functions. While this study aims to optimize for solely dissipation and dispersion characteristics, one may devise situations where stencil sizes may also be considered an additional performance metric (with smaller stencil sizes preferred over larger ones). Indeed, one may also include a-posteriori error estimates as added objective functions to convert this problem to a ‘many-objective’ optimization framework. This proof-of-concept study establishes the first step in including multiple performance criterion for the development and selection of a particular scheme.

The major facets of this investigation may be enumerated in the following:

- A multiobjective optimization problem is framed for a fourth-order convergence accurate finite difference scheme design in a seven-point stencil.
- The NSGA II algorithm is utilized for solving this

R. Maulik is a PhD Candidate in the School of Mechanical & Aerospace Engineering, Oklahoma State University, Stillwater, OK, 74078 USA e-mail:romit.maulik@okstate.edu

G. Yen is MAE 5773 instructor.

framework for constrained optimization. Constraints are imposed solely on the dissipation magnitude at the grid cut-off wavenumber.

- Several schemes with different dissipative tendencies are outlined along with their modified wavenumber analysis [8].
- A sample dissipative scheme is utilized to demonstrate the stabilization of solution fields obtained from the Burgers equation with intense gradients.

II. OPTIMIZATION PROBLEM

In this section we frame the optimization problem that shall be investigated for scheme design. We proceed initially with a Taylor's series based fourth-order numerical scheme for the first order derivative while utilizing a seven-point stencil. Following this a modified wavenumber analysis akin to Lele's approach [1] is utilized to quantify dispersive and dissipative characteristics of the scheme as a function of certain free parameters. These parameters are our decision variables. Further details are provided in the following.

A. First-order derivative stencil

We utilize a seven point stencil in the finite difference sense to calculate the first derivative and follow Tam and Webb's notation [3] to get

$$\frac{\partial u}{\partial x}(x) \approx \frac{1}{\Delta x} \sum_{j=-N}^N a_j u(x + j\Delta x) \quad (1)$$

where we have assumed a uniform finite difference grid with Δx spacing between points. For a 7 point stencil, our choice for N becomes 3 with j chosen as a spatial index for an array type datastructure. A simple Taylor's series expansion [8] of neighboring points around $u(x)$ leads to the following set of equations, which when enforced, satisfy fourth-order convergence in the discrete scheme:

$$a_0 = -10(a_{-3} + a_3) \quad (2)$$

$$a_1 = 5a_{-3} + 10a_3 + \frac{2}{3} \quad (3)$$

$$a_2 = -a_{-3} - 5a_3 - \frac{1}{12} \quad (4)$$

$$a_{-1} = 10a_{-3} + 5a_3 - \frac{2}{3} \quad (5)$$

$$a_{-2} = -5a_{-3} - a_3 + \frac{1}{12}. \quad (6)$$

One can now observe that all the coefficients ($a_i; -2 \leq i \leq 2$) are expressed as a function of two free parameters a_3 and a_{-3} . These are now our decision variables.

B. Modified wavenumber analysis

The previous section has dealt with the process of bounding the order of convergence for the proposed seven point scheme. In the following we utilize the free parameters a_{-3} and a_3 to obtain estimates of dispersive and dissipative behavior for the chosen stencil configuration. For this we utilize the following

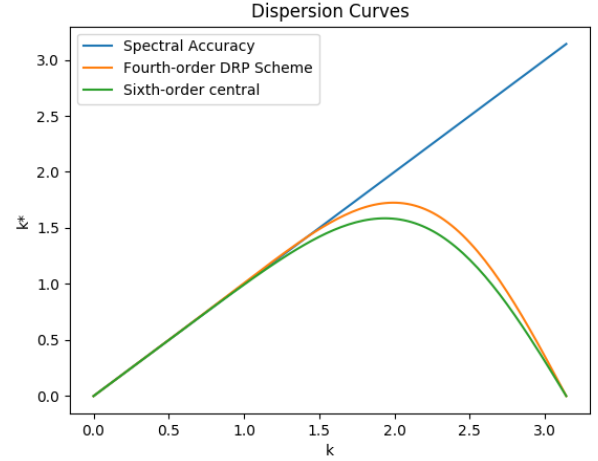


Fig. 1. Dispersive behavior of the fourth-order DRP and sixth-order central schemes. Note that there is zero dissipation.

modified wavenumber analysis. Let us assume a hypothetical solution given by

$$u(x) = e^{ikx} \quad (7)$$

where k corresponds to spatial wavenumbers and $i = \sqrt{-1}$. A spectrally accurate first-order derivative of the above field can be obtained as

$$\frac{\partial u(x)}{\partial x}(x) = ik u(x). \quad (8)$$

Once our discrete stencil is set up we may also represent it in spectral space

$$iku(x) \approx \frac{1}{\Delta x} \sum_{j=-N}^N a_j e^{ik(x+j\Delta x)}, \quad (9)$$

which becomes

$$ik \approx \frac{1}{\Delta x} \sum_{j=-N}^N a_j e^{ik(j\Delta x)}. \quad (10)$$

Comparing the imaginary part of both sides of the above equation gives us curves related to the dispersive performance of the chosen scheme. The real part of the right hand side corresponds to the dissipative behavior and is monotonically increasing for the chosen stencil till the grid cut-off wavenumber. A sample curve showing the sixth-order accurate central scheme (i.e. $a_3 = \frac{1}{60}, a_{-3} = -\frac{1}{60}$) and the fourth-order accurate dispersion relation preserving scheme described by Tam and Webb (i.e. $a_3 = 0.02651995, a_{-3} = -0.02651995$) are shown in Figure 1. We note that both these schemes are central in nature with $a_0 = 0$ leading to zero dissipation.

C. Quantifying scheme performance

On obtaining dispersion and dissipation curves, an L^1 -norm criteria is utilized for assessing the performance of the scheme in terms of closeness to spectral accuracy for dispersion

and dissipative tendencies at various discrete wavenumbers. Mathematically this corresponds to

$$f_1(a_{-3}, a_3) = \sum_{j=1}^{N_k} \frac{1}{k_j} |\text{Im}(k_j^*) - k_j|, \quad (11)$$

for dispersion where a weighting factor of $1/k_j$ is utilized to ensure priority in accuracy is given to higher wavenumbers. Our true (or spectrally accurate) wavenumber is simply k_j (from the left hand side of equation 9) and k_j^* is the modified wavenumber due to discretization (obtained from the right hand side of the same equation). We note that our highest wavenumber k_{N_k} is given by π from the Nyquist sampling criterion. Our second objective function can be framed as

$$f_2(a_{-3}, a_3) = \sum_{j=1}^{N_k} |\text{Re}(k_j^*)|. \quad (12)$$

With this our optimization problem can be formally set up as

$$\min\{[f_1, -f_2] \cong f(a_{-3}, a_3) : \text{Constraints}\}. \quad (13)$$

For this study, our constraints are given by an invalid solution if dissipation is greater than an a-priori specified value. It will be demonstrated later, that the specification of this tolerance leads to unique scheme selections by our choice of an intelligent multiobjective optimization algorithm.

III. MULTIOBJECTIVE OPTIMIZATION: NSGA II

In this section we outline the famous NSGA II algorithm [7] for our multiobjective optimization purposes. Code and supporting material may be found online on the author's Github repository. There are three primary elements of the NSGA II algorithm. These are

- 1) A fast-non-dominated-sort.
- 2) A crowding distance assignment.
- 3) Genetic evolution through crossover and mutation.

In the above list, item 1 pertains to the elitism preservation procedure for this evolutionary strategy. The crowding distance assignment ensures diversity in the pareto-front and the operations of crossover and mutation ensure a wide search for increasingly optimal solutions through successive iterations. The procedure of the fast-non-dominated-sort (FNDS) is necessary for the identification of solutions which may be considered to be closest to the pareto-front. Indeed, the FNDS procedure leads to a segregation of solutions into successive fronts (which are progressively further than the pareto region). Figure 2 displays a two-objective minimization situation (i.e. where both dispersive and dissipative error are minimized) and a snapshot of the first three fronts obtained from FNDS. The pseudocode for the FNDS algorithm is given in Algorithm 1. Following FNDS a diversity preserving crowding sort is implemented through Algorithm 2 where an additional fitness is prescribed on the basis of a crowding distance assignment (CDA). This is to ensure that solutions do not cluster near each other and can be visually seen in Figure 3 where lower values of crowding distances are in less diverse regions. Finally a genetic algorithm based evolution is carried out on the

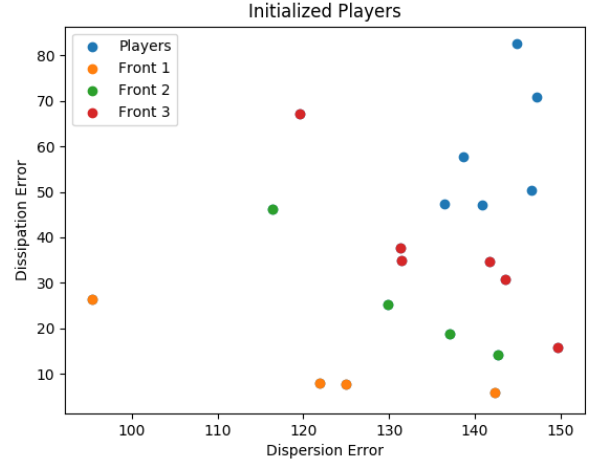


Fig. 2. The first three fronts from an FNDS for a two-objective minimization problem

Algorithm 1 Fast-non-dominated-sort (FNDS) for a population P

```

1: for  $p \in P$  do
2:    $S_p = \Phi, n_p = 0$  {Initialize dominated set and counter}
3: for  $q \in P$  do
4:   if  $p < q$  {If p dominates q} then
5:      $S_p = S_p \cup q$  {Add q to dominated set}
6:   else
7:      $n_p = n_p + 1$  {Increment domination counter}
8:   end if
9: end for
10: if  $n_p = 0$  {p belongs to first front} then
11:    $prank = 1$ 
12:    $\mathcal{F}_1 = \mathcal{F}_1 \cup \{p\}$ 
13: end if
14: end for
15:  $i = 1$  {Initialize the front counter}
16: while  $\mathcal{F}_i \neq \Phi$  do
17:    $Q = \Phi$  {Store members of next front}
18:   for  $p \in \mathcal{F}_i$  do
19:     for  $q \in S_p$  do
20:        $n_q = n_q - 1$ 
21:       if  $n_q = 0$  {q belongs to the next front} then
22:          $qrank = i + 1$ 
23:          $Q = Q \cup \{q\}$ 
24:       end if
25:     end for
26:   end for
27:    $i = i + 1$ 
28:    $\mathcal{F}_i = Q$ 
29: end while

```

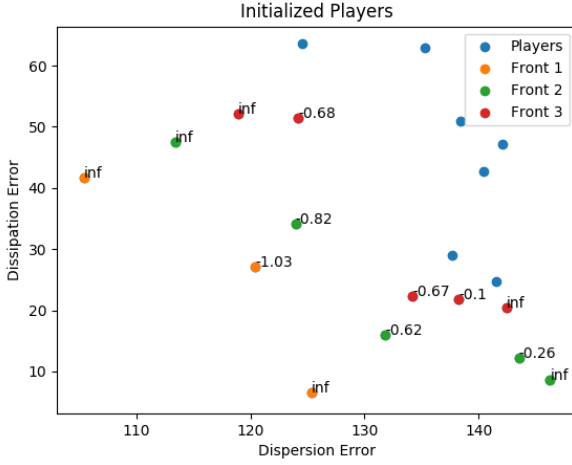


Fig. 3. Crowding distance assignments for the first three fronts for a two-objective minimization problem. Note how boundary points are infinity and crowded locations have lower values.

Algorithm 2 A crowding-distance-assignment (CDA) for a front I .

- 1: $l = |I|$ {Number of solutions in I }
- 2: **for** $i \in I$ **do**
- 3: Set $I[i]_{dist} = 0$ {Initialize distance}
- 4: **end for**
- 5: **for** Each objective m **do**
- 6: $I[1]_{dist} = I[l]_{dist}$ {Largest priority to boundary points}
- 7: **for** $i = 2$ to $(l - 1)$ {All other points} **do**
- 8: $I[i]_{dist} = I[i]_{dist} + \frac{I[i+1] - I[i-1]}{f_m^{max} - f_m^{min}}$
- 9: **end for**
- 10: **end for**

principles of cross-over and mutation as shown in Algorithm 3.

To test the implementation of the aforementioned algorithms, we test our NSGA II optimizer for the Fonseca and Fleming test function [9]. A plot comparing the pareto-fronts obtained by our implementation and the truth are shown in Figure 4. A good match is observed which ensures that our optimizer performs to our basic expectation.

IV. RESULTS

In the following section we outline the results for our optimization in terms of customized dissipation schemes ob-

Algorithm 3 Genetic algorithm based population evolution.

- 1: $P_o = \Phi, P_p = P$ {Set up parent and offspring populations}
- 2: $x_n = 3, m_r = 0.1$ {Simulated binary crossover and mutation rate parameters.}
- 3: Perform crossover operations to get P_o of equal size as P_p
- 4: Perform mutation operations on P_o
- 5: Total new population $P_{new} = P_p + P_o$ ready for FNDS and CDA.

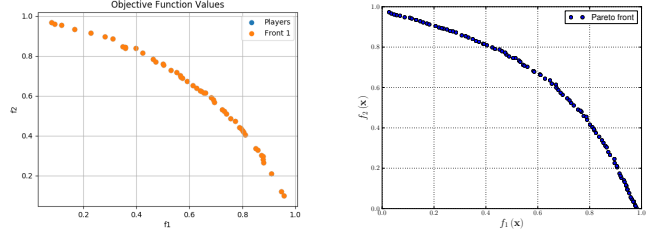


Fig. 4. Validation of NSGA II implementation with Fonseca and Fleming function. The plot on the right shows the true pareto-front.

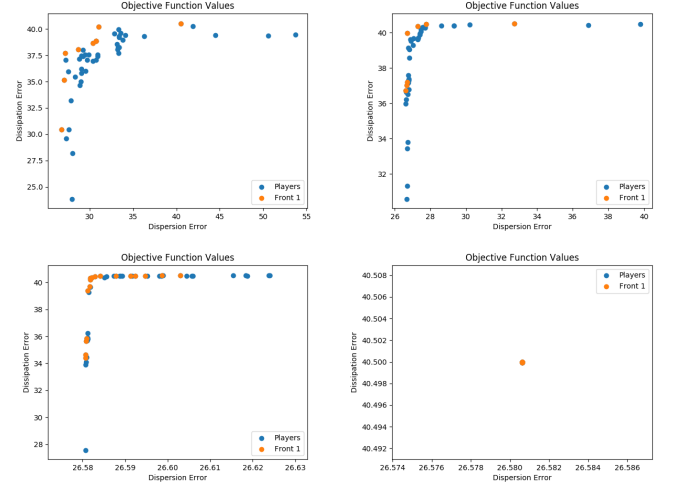


Fig. 5. Progress to pareto-optimality for given problem. Note convergence to a single optimal point.

tained using the aforementioned strategy. A sample customized scheme is then implemented into a viscous Burgers equation evolution to ensure that the additional dissipation stabilizes numerical oscillations at vicinities of high gradients.

A. Progress to optimality

An interesting observation in the due course of this study was that of a ‘zero-dimensional’ pareto-front. A single optimal value was obtained for a specified dissipation constraint (refer Equation 13) irrespective of the number of players or spread of initialization. In hindsight, this is evidence that the process of framing the dispersion and dissipation problem as two separate objectives could be replaced by a single *constrained* objective optimization (which shall be a subject of future investigations). Figure 5 shows the progress to optimality for a desired value of the dissipation constraint. A fortunate byproduct of this behavior is a *repeatability* in the outcome of this optimization problem. Given a particular value of the dissipation constraint, the same numerical scheme was obtained (down to machine precision).

B. Schemes obtained

Multiple optimization problems were solved with different values of the dissipation constraint to obtain different finite difference schemes. These are outlined in Table I. Dissipation and

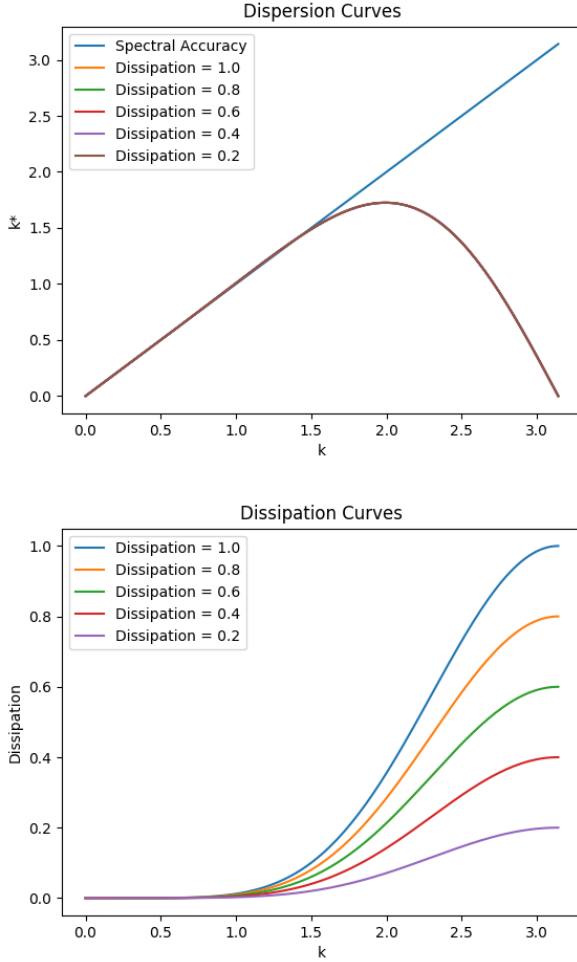


Fig. 6. Dispersion (top) and dissipation (below) characteristics of schemes obtained through proposed optimization framework.

dispersion behavior of the obtained spectra are also described visually through Figure 6. An interesting observation is that the choice of dissipation does not affect the dispersion behavior of the discretization which possibly ties into the fact that the proposed framework may be framed as a single objective problem. Another interesting feature is the purely monotonic behavior of the dissipation curve. In effect, this implies that the choice of the dissipation constraint completely determines the varying dissipation with the wavenumber. We note that all the optimizations were carried out with a population size of 50 players, a simulated binary crossover parameter of 3 and a mutation rate of 0.1.

C. Viscous Burgers equation

For a final validation of the developed schemes, we utilize them in an a-posteriori simulation of the viscous Burgers equation. This system can be expressed as

$$\begin{aligned} \frac{\partial u}{\partial t} + \frac{1}{2} \frac{\partial u^2}{\partial x} &= \nu \frac{\partial^2 u}{\partial x^2}, \\ u &\rightarrow u(x, t) \in \mathbb{R}. \end{aligned} \quad (14)$$

In particular we use a periodic one-dimensional domain with a viscosity given by $\nu = 5 \times 10^{-4}$ and resolution of 512 grid points. Further details of the computational implementation of this problem along with detailed discussion of the initial conditions chosen are available in [10]. It is well known that the viscous Burgers equations is a viable preliminary framework for numerical scheme testing prior to deployment in full-blown conservation laws due to its quadratic nonlinearity and hyperbolic character in the limit of vanishing viscosity. We note that the discretization of the viscous term on the right hand side the conservation law uses a standard fourth-order Padé scheme to ensure variation in results are solely as a result of our choice of scheme for the first-order derivative for the nonlinear term. Figure 7 shows the stabilization affect of the added dissipation due to the $d = 0.6$ constraint scheme. For the purpose of comparison we include the fourth-order accurate DRP scheme of Tam and Webb with no dissipation. This indicates the possibility of a parameter dependent LES framework which may be explored for the purpose of parameter based implicit turbulence modeling. To the best of this author's knowledge, most implicit turbulence models are 'hard-coded' in that the dissipation cannot be varied dynamically through time integration. In terms of wavenumber capture, a spectrally averaged kinetic energy spectra is shown in Figure 8 where our devised scheme recovers the theoretical scaling of k^{-2} expected from the viscous Burgers equation showing significant high wavenumber content. Our next step in this investigation is to replicate this study for more challenging flows such as the Taylor-Green vortex test case. Another interesting study would be to check at what levels of dissipation we begin to recover shock capturing behavior for purely hyperbolic systems of equations.

V. CONCLUDING REMARKS

In this study we have set up the problem of numerical scheme design as a multiobjective evolutionary optimization study. To that end, a seven point stencil limited to fourth-order truncation accuracy is chosen with two model coefficients as free parameters. Our objective functions are determined using an L^1 -norm based loss function from the modified wavenumber analysis of our discretized schemes which display the dispersive and dissipative errors induced due to Taylor's series approximations. Our multiobjective optimization strategy uses NSGA-II for pareto-front search and our implementation is validated for the Fonseca and Fleming function. It is observed that various choices of our dissipation constraint determine repeatable outcomes of a pareto-front that consists of a single point implying that the multiobjective function can be framed as a constrained single objective system. Various choices of the dissipation parameter result in different finite difference schemes with the dissipation constraint magnitude being achieved at the grid cutoff wavenumber π . To test our formulation in an a-posteriori setting we utilized the viscous Burgers equations which is a one-dimensional prototype of the full Navier-Stokes equations with a quadratic nonlinearity and hyperbolic behavior in the limit of vanishing viscosity. Our dissipative schemes are seen to stabilize the evolution

TABLE I
A REPRESENTATION OF THE VARIOUS SCHEMES OBTAINED FROM THIS STUDY

Dissipation	a_0	a_{-1}	a_{-2}	a_{-3}	a_1	a_2	a_3
0.2	0.0625	-0.846141417	0.208163133	-0.02964495	0.752391417	-0.170663133	0.02339495
0.4	0.125	-0.893016417	0.226913133	-0.03276995	0.705516417	-0.151913133	0.02026995
0.6	0.1875	-0.939891417	0.245663133	-0.03589495	0.658641417	-0.133163133	0.01714495
0.8	0.25	-0.986766417	0.264413133	-0.03901995	0.611766417	-0.114413133	0.01401995
1	0.3125	-1.033641417	0.283163133	-0.04214495	0.564891417	-0.095663133	0.01089495

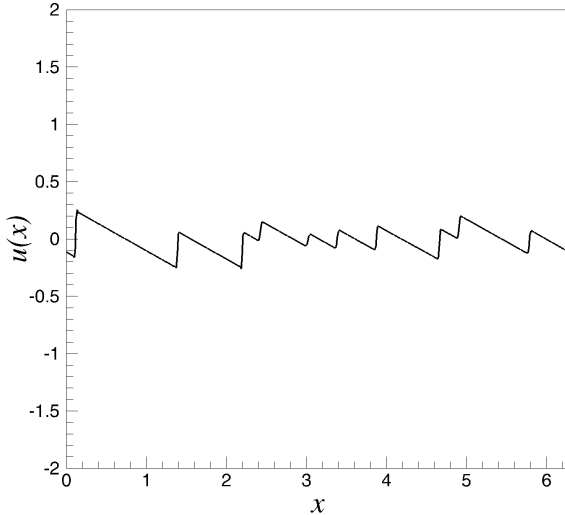
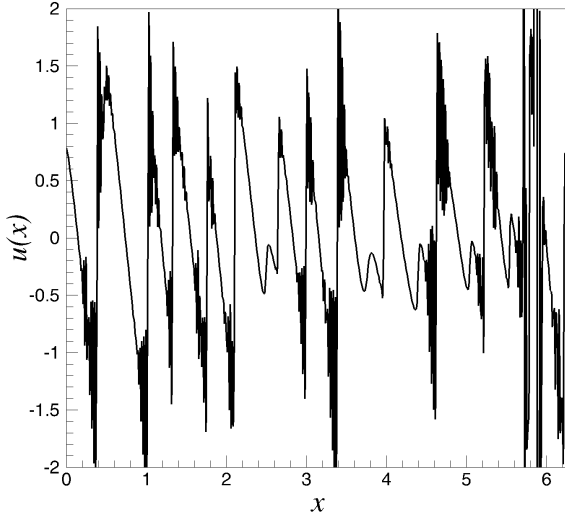


Fig. 7. Results for the simulation of the viscous Burgers equation with non-dissipative (top) and customized dissipation (bottom) schemes.

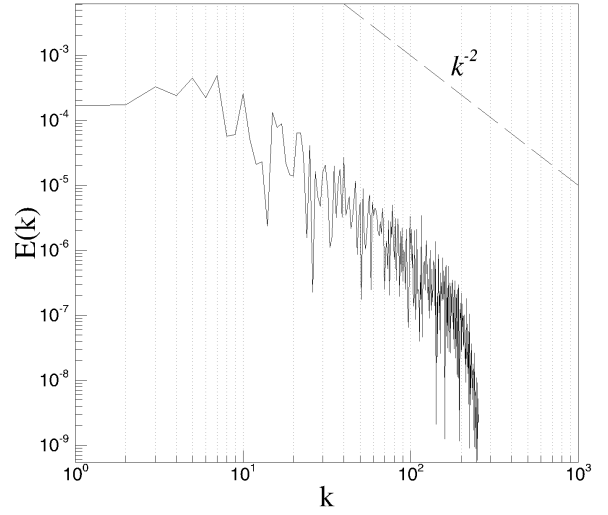


Fig. 8. Spectrally averaged kinetic energy spectra for the viscous Burgers equation solution obtained by the proposed framework for scheme design.

of the Burgers equations successfully by smoothing any numerical oscillations in the vicinity of sharp gradients formed. This is also observed in kinetic energy spectra where the theoretical scaling of the k^{-2} for Burgers equation exhibiting scale separation is obtained without any aliasing error due to numerical oscillations. Results indicate a promising framework for scheme design through looking at a-priori error estimates. In terms of promise, this gradient free approach represents an opportunity to integrate a-posteriori error estimates into scheme design choices particularly for flow situations where complicated geometries and turbulence nonlinearities may require customized dispersion and dissipation behavior. In that sense, the presented study represents a proof-of-concept for a scheme design framework that requires the specification of multiple competing objectives from the end-users point of view. Future investigations will study pareto-front capture for flows with ‘engineering’ objective functions integrated into multiobjective framework.

ACKNOWLEDGMENT

The author would like to thank Dr. Gary Yen for the many excellent conversations initiated in the Intelligent Systems and Stochastic Systems courses. In addition, the author appreciates the guidance of Dr. Omer San in the preparation of this study.

REFERENCES

- [1] S. K. Lele, "Compact finite difference schemes with spectral-like resolution," *J. Comp. Phys.*, vol. 103, no. 1, pp. 16–42, 1992.
- [2] J. W. Kim and D. J. Lee, "Optimized compact finite difference schemes with maximum resolution," *AIAA J.*, vol. 34, no. 5, pp. 887–893, 1996.
- [3] C. K. W. Tam and J. C. Webb, "Dispersion-relation-preserving finite difference schemes for computational acoustics," *J. Comp. Phys.*, vol. 107, no. 2, pp. 262–281, 1993.
- [4] P. Sagaut, *Large eddy simulation for incompressible flows: an introduction*. Springer Science & Business Media, 2006.
- [5] A. N. Kolmogorov, "The local structure of turbulence in incompressible viscous fluid for very large reynolds numbers," in *Dokl. Akad. Nauk SSSR*, vol. 30, no. 4, 1941, pp. 299–303.
- [6] F. F. Grinstein, L. G. Margolin, and W. J. Rider, *Implicit large eddy simulation: computing turbulent fluid dynamics*. Cambridge university press, 2007.
- [7] K. Deb, A. Pratap, S. Agarwal, and T. Meyarivan, "A fast and elitist multiobjective genetic algorithm: NSGA-II," *IEEE Trans. Evol. Comput.*, vol. 6, no. 2, pp. 182–197, 2002.
- [8] P. Moin, *Fundamentals of engineering numerical analysis*. Cambridge University Press, 2010.
- [9] C. M. Fonseca and P. J. Fleming, "An overview of evolutionary algorithms in multiobjective optimization," *Evol. Comput.*, vol. 3, no. 1, pp. 1–16, 1995.
- [10] R. Maulik and O. San, "Explicit and implicit LES closures for burgers turbulence," *J. Comp. Appl. Math.*, vol. 327, pp. 12–40, 2018.